Colloid and Polymer Science (2022) 300:1113–1127
https://doi.org/10.1007/s00396-022-04994-y

ORIGINAL CONTRIBUTION

Polycarboxylate ether superplasticizer with gradient structure: excellent dispersion capability and sulfate resistance

Xiya Fang[1] · Yan Shi[1] · Chunfu Yan[2] · Honggen Wang[1] · Jia Hui[3]

Received: 26 January 2022 / Revised: 11 May 2022 / Accepted: 25 May 2022 / Published online: 10 August 2022

Abstract

In this paper, gradient and block polycarboxylate ether superplasticizers (PCEs) composed of allyl alcohol polyoxyethylene ether macromonomer and acrylic acid were synthesized via aqueous reversible addition-fragmentation chain transfer (RAFT) polymerization. The molecular structure of PCEs was characterized by ^{1}H nuclear magnetic resonance (NMR), Fourier transform infrared (FT-IR) spectroscopy, and size exclusion chromatography (SEC), and the fluidity of cement paste and the influence of SO_4^{2-} on the dispersibility of PCEs were investigated in detail. The experimental results show that the molecular weight and polydispersity of the obtained PCEs were well controlled by the RAFT process. Compared with the PCEs prepared by conventional free radical polymerization, the gradient PCEs synthesized by RAFT polymerization exhibited excellent dispersion capability. The range of molecular weights and acid-ether ratios of the gradient PCEs for high fluidity of cement paste was much wider. Furthermore, PCEs with gradient structure also showed excellent sulfate resistance. In contrast, PCEs with block architecture exhibited the lowest flowability. Based on these findings, the relationship between dispersibility of PCEs and their chemical structures was illustrated.

Keywords Polycarboxylate ether (PCE) · Superplasticizer · RAFT polymerization · Gradient copolymer · Block copolymer

Introduction

As a widely used building material, chemical admixtures are in high demand in concrete industry to enhance their performance including durability, flowability, mechanical properties, and so on [1–3]. As one of the most important admixtures, superplasticizers are mainly used to decrease the initial amount of water added for good flowability of cement paste [4]. This decrease in water content (or increase in solid volume fraction) leads to a decrease in the porosity of the hardened material and produces a more durable concrete with better mechanical performances [5]. Polycarboxylate ether (PCE) is a new generation of superplasticizer, which was invented in 1981 [6], following the development of conventional lignosulfonate water reducing agent, naphthalene, and melamine-based superplasticizers. Owing to the presence of both carboxylic groups and poly (ethylene oxide) (PEO) side chains [7, 8], comb-like PCE copolymers can induce both electrostatic repulsion and steric hindrance, thus providing better performance than previous generations, such as high water-reduction ratio, long slump retention time and environmental friendliness [9–12]. Therefore, polycarboxylate ether superplasticizers (PCEs) is now being more and more widely used in concrete technology [13].

Conventional free radical polymerization (FRP) is the main synthetic method for the synthesis of industrial PCEs. Although FRP is extensively employed to prepare PCE superplasticizers, the control over molecular weight and molecular weight distributions of PCE copolymers is very weak. Polydispersity index (PDI) values of PCE are usually higher than 1.5 even when chain transfer agents are used to mediate the copolymerization process, and the wider molecular weight distributions make it hard to evaluate the

✉ Yan Shi
shiyan@mail.buct.edu.cn

✉ Chunfu Yan
yancfgfz10@126.com

[1] State Key Laboratory of Organic-Inorganic Composites, Beijing University of Chemical Technology, Beijing 100029, People's Republic of China

[2] Hebei Shuangcheng Construction Engineering Testing Co, Ltd, Hebei 050031, People's Republic of China

[3] Engineering Technology and Materials Research Center, China Academy of Transporting Sciences, Beijing 100029, People's Republic of China

relationship between the structure (including molecular weight) of PCEs and the properties of plasticized cement paste. In addition, the comonomer reactivities vary greatly and the copolymer chains are instantaneously formed in FRP, leading to great differences in copolymer composition and structure in different reaction periods [14], thus it becomes even harder to explore the relationship between the chemical compositions of PCEs and performances of cement product. As a robust and versatile controlled/living free radical polymerization technique, reversible addition-fragmentation chain transfer (RAFT) polymerization is compatible with a wide range of monomers, including acrylic acid [15, 16], vinyl acetate [17–19], and ethylene [20, 21], which cannot be effectively controlled by other controlled radical polymerization pathways. Besides, diverse reaction media, including water and many polar media, can be employed as media for RAFT polymerization. Many homopolymers or copolymers with well-defined structure and narrow molecular weight distribution have been synthesized by RAFT polymerization [22–25]. We have synthesized several copolymers and copolymer nano-particles containing acrylic acid (AA) segments by RAFT polymerization in the past few years [26, 27].

Gradient copolymers are a special kind of copolymers with unique main-chain structure, in which the monomer composition changes gradually from one end of the polymer chain to the other [28]. Such polymers exhibit broad glass transitions, which are useful in shock and noise-absorbing materials [29]. In addition, gradient copolymers possess improved interfacial stabilizing effect compared to block copolymers [30, 31], and some scholars have confirmed that gradient copolymers have a better dispersing performance than analogous block or statistical copolymers [32, 33]. Sika Technology reported the synthesis of gradient copolymers consisting of PEG methacrylate/methacrylic acid (PEGMA/MAA) via RAFT polymerization, which were used as dispersing agents for construction material applications. Their results showed that the gradient copolymer provided a better dispersion of cement particles than the random copolymer analogs. Gradient character was used to describe the copolymer, nevertheless the structure and composition of the copolymer was not fully characterized. Pourchet and co-workers also synthesized a novel kind of gradient PCEs by RAFT copolymerization of PEGMA with MAA. They proved that the "gradient" PCEs are less sensitive to sulfate competitive adsorption than "random" PCEs [34]. Similarly, the gradient structure of PCEs was not characterized. Moreover, intermittent feeding strategy was utilized to prepare the gradient copolymer, so the gradient structure of this copolymer thus formed is not well-defined theoretically. Furthermore, it is generally recognized that ester groups are susceptible to hydrolysis, and therefore, the performance of ester-based PCEs is not as good as that of ether-based PCEs [35].

Mi and co-workers used AA and methyl allyl alcohol polyoxyethylene ether (TPEG) as comonomers to prepare PTPEG-*b*-PAA-*b*-PTPEG triblock copolymer through three-step RAFT polymerization in n-propanol [36]. They investigated the effects of molecular weight and acid-ether ratio on the performance of PCEs. Yu and co-workers prepared BAPP-AA-BAPP triblock PCEs through RAFT copolymerization of butenyl alkylene polyoxyethylene-polyoxypropylene ether (BAPP) macromonomer and AA in n-propanol, and the effect of acid-ether ratio on the performance of PCEs was also investigated [37]. Yu believed that these triblock structured PCEs can adsorb on cement particles much stronger than random PCEs, but the author did not provide comparison results. These block polymerizations were all carried out in organic solvents, therefore, the PCE products cannot be used in concrete directly. Post-processing is required to eliminate the organic solvent and get PCE for practical application, which is very troublesome and time-consuming. Meanwhile, as the reactivities of TPEG or BAPP macromonomers were much less than AA, the homopolymerization of these two macromonomers was extremely difficult to achieve, hence the block copolymerization of these macromonomers may be problematic.

Based on the above discussion, the synthesis of PCEs by aqueous RAFT polymerization is a very meaningful research topic because the PCE products can be applied directly to cement or concrete. In addition, the previous research works have shown that the dispersion ability of gradient and block PCEs is better than the random copolymer analogs. However, there are scarce data concerning the comparison between gradient and block PCEs, which has important implications for the design and application of high-performance PCEs.

In this study, PCEs composed of TPEG macromonomer and AA were synthesized via RAFT polymerization in aqueous solution. The molecular structures of the obtained PCEs were analyzed by ^{1}H nuclear magnetic resonance (^{1}H-NMR) and Fourier transform infrared (FT-IR) spectroscopy. The molecular weight of the resultant PCEs determined by size exclusion chromatography (SEC) showed narrower distribution as compared with the random copolymer analogs prepared by FRP. To further study the effect of molecular structure on the properties of PCEs, gradient and two kinds of block PCEs were specially designed and synthesized, and compared with the random analogs prepared by FRP. It is found that PCEs with gradient structure exhibit the best dispersion properties and sulfate resistance in comparison with the block and random analogs. At the same time, the influence of molecular weight and acid-ether ratio on the performance of gradient PCEs was also studied in detail.

Materials and methods

Materials

AA (99%, Tianjin fuchen chemical plant) was distilled under reduced pressure prior to use. Tetrabutylammonium bromide (Merck), chloroform (Guide chemical), acetone (Aladdin), sodium hydroxide (Aladdin), carbon disulfide (Aladdin), 2,2′-Azobis[2-(2-imidazolin-yl) propane] dihydrochloride (VA0-44, Aladdin), sodium sulfate (Na_2SO_4, Aladdin), thioglycolic acid (TGA, Beijing Innochem), trioxane (Shanghai Mackin Biochemical Co., Ltd.), concentrated hydrochloric acid (HCl, Beijing Tong Guang Fine Chemicals Company), and concentrated sulfuric acid (Beijing Tong Guang Fine Chemicals Company) were used as received. Deionized water was used in the present study.

TPEG (Liaoning Kelong Fine Chemical Co., Ltd.) is methyl allyl alcohol polyoxyethylene ether and the number-average molecular weight ($\overline{M}_n$) is 2400 g/mol.

Commercial PCEs (Blank) was purchased from Jiangsu Subote New Material Co., Ltd.

P·I42·5 Portland cement, complying with the Chinese national standard GB 8076–2008 (SAC, 2008a), was supplied by China Building Materials Academy. Its chemical and mineral composition are listed in Table 1.

Synthetic process

Synthesis of S, S′-Bis (α, α′-dimethyl-α′′-acetic acid)-trithiocarbonate

In this paper, bifunctional S, S′-Bis (α, α′-dimethyl-α′′-acetic acid)-trithiocarbonate (BDMAT) was used as the RAFT reagent, and the synthesis of BDMAT is mainly carried out according to the literature [38]. The synthetic steps are as follows: carbon disulfide (27.4 g, 0.36 mol), chloroform (107.5 g, 0.9 mol), acetone (52.3 g, 0.9 mol), and tetrabutylammonium bromide (2.29 g, 7.1 mmol) were mixed with 120 mL of acetone in a 2 L jacketed reactor cooled with tap water under nitrogen. Sodium hydroxide (50%) (201.6 g, 2.52 mol) was added dropwise over 90 min to keep the temperature below 25 °C. The reaction mixture was stirred overnight. Nine hundred milliliters of water was then added to dissolve the solid, followed by 120 mL of concentrated HCl to acidify the aqueous layer. Then the solution was stirred for 30 min with nitrogen purge, filtered and rinsed the solid thoroughly with water. The solid was dried at 40 °C to constant weight.

Synthesis of PCEs by RAFT polymerization

Using BDMAT as RAFT agent, VA0-44 as initiator and water as the solvent, we synthesized PCEs by aqueous RAFT polymerization. For a typical synthetic process of the gradient PCE, TPEG, VA0-44, and BDMAT were dissolved in water in a 100 mL Schlenk flask with a magnetic stirring bar. The solution was purged with argon for 30 min and then heated to 60 °C in an oil bath. Subsequently, AA aqueous solution was fed into the flask dropwise in 2 h. After completion of dropping, the solution was kept stirring at 60 °C for 3 h. During the polymerization process, samples were extracted with syringe for characterizations at certain time intervals.

For the synthesis of PCE with block structure, the overall molar ratio of AA:TPEG was kept at 6:1. Half the amount of AA was copolymerized with TPEG to get the P(AA-*grad*-TPEG) block, and the other half was used to form the pure PAA block, then PCE with P(AA-*grad*-TPEG)-*b*-PAA-*b*-P(AA-*grad*-TPEG) block structure was obtained. The preparation process of the P(AA-*grad*-TPEG) block is the same as the above mentioned method for gradient PCE. After AA and TPEG were consumed completely (determined by ^{1}H-NMR spectrum), P(AA-*grad*-TPEG)-based trithiocarbonate macro-RAFT agent (abbreviated as P(AA-*grad*-TPEG)-TTC-P(AA-*grad*-TPEG)) was obtained. In the second step, the remaining AA monomer was added to the reaction flask and reacted for another 5 h. Then, P(AA-*grad*-TPEG)-*b*-PAA-*b*-P(AA-*grad*-TPEG) was obtained.

For the synthesis of PAA-*b*-P(AA-*grad*-TPEG)-*b*-PAA, the pure PAA block at both ends was prepared first and the P(AA-*grad*-TPEG) block was formed in the second step. The operation procedures of the two steps were identical to those of P(AA-*grad*-TPEG)-*b*-PAA-*b*-P(AA-*grad*-TPEG).

Synthesis of PCEs by conventional FRP

Using thioglycolic acid (TGA) as chain transfer agent, VA0-44 as initiator and water as the solvent, PCEs with different molar ratio of acid:ether and molecular weight were synthesized by FRP. The specific preparation process is as follows: First, TPEG was dissolved in water in a flask. The aqueous solution of VA0-44 and TGA was used as solution A, and the aqueous solution of AA was used as solution B. Then the solution A and solution B were dripped separately and simultaneously into the flask using peristaltic pump, and the dripping time was 2 h. After completion of the addition, the solution was stirred steadily for 3 h.

Table 1 Chemical and mineral composition of the cement

SiO_2	Al_2O_3	Fe_2O_3	CaO	MgO	SO_3	Na_2Oeq	f-CaO	C_3S	C_2S	C_3A	C_4AF
20.3	5.42	3.99	63.43	2.03	0.97	0.52	0.87	58.99	14.02	7.62	12.13

Structural characterizations

Fourier transform infrared (FT-IR) spectroscopy

The samples were measured by Bruker Tensor II FT-IR spectrometer. The samples were prepared by KBr tablet method, and the spectra were observed in the range of 4000 ~ 400 cm^{-1}. The test resolution was 4 cm^{-1}.

^{1}H nuclear magnetic resonance (NMR) spectroscopy

The ^{1}H-NMR spectra were recorded on a superconducting magnet NMR spectrometer (Bruker Avance III 400 MHZ), and the samples were dissolved in DMSO or $CDCl_3$. Tetramethylsilane (TMS) was used as an internal reference.

Size exclusion chromatography (SEC)

Molecular weight and molecular weight distribution of PCEs were measured by a SIL-20A Shimadzu SEC. SEC test temperature is 40 °C, and 0.1 M NaCl aqueous solution was adopted as the mobile phase with the flow rate of 0.5 mL/min. The concentration of the sample solution is 2 mg/mL, and all sample solutions were filtered with a 0.25 μm filter membrane prior to the test. Calibration is using different molecular weight low-dispersion dextran standards.

Fluidity of cement paste

The fluidities of cement slurries were measured according to the Chinese standard GB/T 8077–2012 [39]. Generally, the water with certain amount of PCEs was added to cement with a water/cement ratio (W/C) of 0.29, and the dosage of dispersant was 0.15% (weight percent of cement). After being mixture thoroughly, the cement pastes were poured into a truncated cone placed on a glass plate, and then the cone was vertically removed. The spread diameter of the cement slurry was recorded after flowing for 30 s, which was the average value of two perpendicular measurements.

Adsorption measurements

The adsorbed amount of PCEs per unit mass of cement was determined from the total amount of organic carbon (TOC) in solution using the depletion method. A TOC analyzer (Vario TOC select, Germany) was used to measure the TOC content of the non-adsorbed portions of the copolymers before and after the adsorption equilibrium of PCEs in cement paste. A series of PCE solutions with different concentration were prepared in advance. Then, the PCEs solution (20.0 g) and cement (1.0 g) were mixed and stirred for 5 min. After that, the suspension was separated by centrifugation at 3000 r/min for 15 min. A clear supernatant was then decanted and filtered through a 0.45 μm filter membrane. Concentrated sulfuric acid is added into the pore solution to remove inorganic carbon (IC) (2% relative to supernatant solution). The supernatant solution was subsequently diluted with deionized water to a proper concentration for TOC measurement. The adsorbed amount of copolymer per unit mass of cement was calculated from the difference between the total TOC content in PCEs solution and free TOC content in the resulting supernatant. The measurements were repeated three times, and the final adsorbed amount was the average value.

Sulfate resistance test

The content of Na_2SO_4 was set to be 0.33%, 1.00%, and 1.67% of cement mass, respectively. Na_2SO_4 was dissolved in water and added to the cement paste with PCEs, and then the fluidity of the cement paste was measured.

Results and discussion

Synthesis of PCEs with well-defined structure

Using structurally symmetrical BDMAT as chain transfer agent, PCEs with different structures were designed and synthesized via copolymerization of TPEG macromonomer and AA in water, as depicted in Fig. 1.

Figure 1a shows the synthetic route of PCE with gradient structure. In AA-TPEG copolymerization system, the reactivity ratio of TPEG is much smaller than that of AA. Specifically, the reactivity ratio of TPEG is close to 0, while the reactivity ratio of AA is about 1.5 [40, 41]. This reactivity ratio suggests that TPEG can hardly homo-polymerize, but prefers to copolymerize with AA. Consequently, block copolymer containing pure polyTPEG block cannot be prepared theoretically. As described in the introduction, copolymers with gradient structure have excellent dispersing properties as compared with random and block copolymers [32, 33]. Therefore, a novel kind of PCE with gradient structure was designed and synthesized according to Fig. 1a by RAFT polymerization. In our present work, AA is added dropwise to the reaction solution containing TPEG, initiator, and BDMAT chain transfer agent. Since the continuous consumption of macromonomer TPEG, the content of TPEG units in the copolymer composition is gradually reduced. At the same time, AA is added dropwise to induce a monomer composition drift, that is, the relative content of AA in the system increases with the reaction proceeding, so the content of AA units in the copolymer is gradually increased with the proceeding

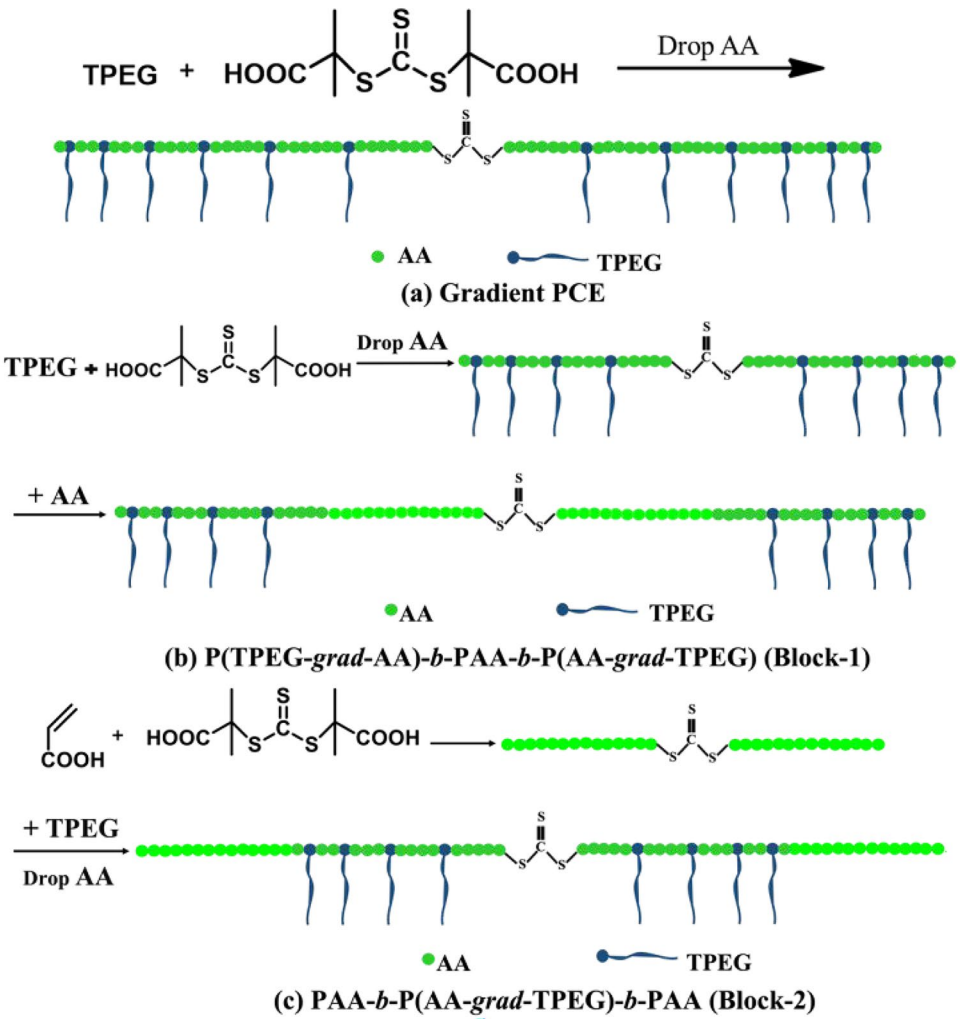

Fig. 1 Schematic representation of the RAFT polymerization for the synthesis of **a** gradient PCE, **b** P(AA-*grad* -TPEG)-*b*-PAA-*b*-P(AA-*grad*-TPEG), and **c** PAA-*b*-P(AA-*grad* -TPEG)-*b*-PAA

of polymerization. Due to the "living" character of the propagating macromolecular chain, the change of copolymer composition was recorded from the α-terminal to the ω- ends. As a result, PCE with gradient structure will be formed, as shown in Fig. 1a.

At the same time, we also designed two kinds of PCE copolymers with block structure in order to verify the influence of molecular structure on the performance of PCE. One is P(AA-*grad*-TPEG)-*b*-PAA-*b*-P(AA-*grad*-TPEG) (Fig. 1b): First, the TPEG monomer was added into the reaction flask, and half the amount of AA monomer was dropped into the reaction system to realize copolymerization with TPEG to form the P(AA-*grad*-TPEG) block. Then another half of AA monomer was added into the reaction flask, and the middle PAA segment was generated. The other one is PAA-*b*-P(AA-*grad*-TPEG)-*b*-PAA, as shown in Fig. 1c, in which an opposite polymerization sequence was adopted: PAA block was formed first, and the middle P(AA-*grad*-TPEG) segment was generated secondly.

PCE with gradient structure

PCE with gradient structure was prepared by "one pot" method according to the procedure described in the "Synthesis of PCEs with well-defined structure" section. A PCE with the AA to TPEG molar ratio of 4:1, which is the most common ratio among PCEs, was prepared first. The dropping time of AA was set as 4 h, and several samples were taken during the reaction. The conversion of AA and TPEG are calculated by ^{1}H-NMR spectra and structure of the macromolecule was analyzed accordingly.

$$\mathrm{Con(AA)} = \frac{\frac{n(AA)}{4} \times t - 2 \times \frac{I_{(a+b+c)}}{I_{5.1}} \times n_{(\mathrm{trioxane})}}{n_{(AA)}} \quad (1)$$

Figure 2 presents the ^{1}H-NMR spectra of the PCE samples during the polymerization process. Peaks a, b, and c are corresponding to three hydrogens on the double bond of AA, respectively ($C\mathbf{H}_2=C\mathbf{H}$). The conversion of

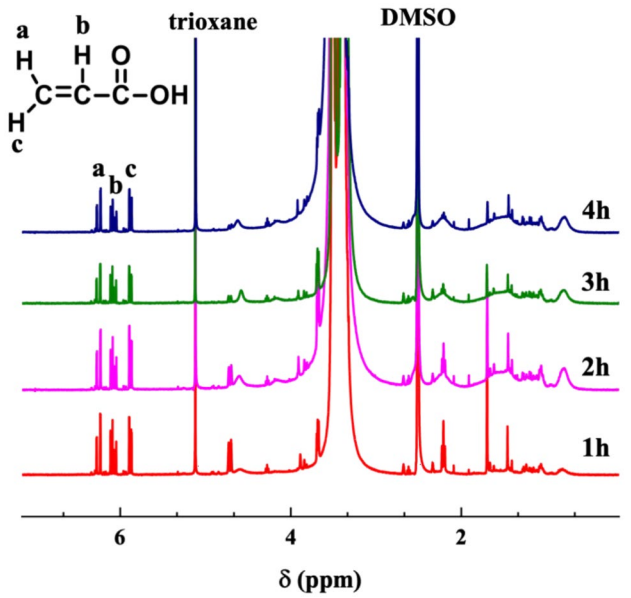

Fig. 2 [1]H-NMR spectra of the PCE during the polymerization process. Solvent: DMSO. Reaction conditions: [AA]: [TPEG]: [BDMAT] = 36:9:0.6, solid content is about 50%, T = 60 °C

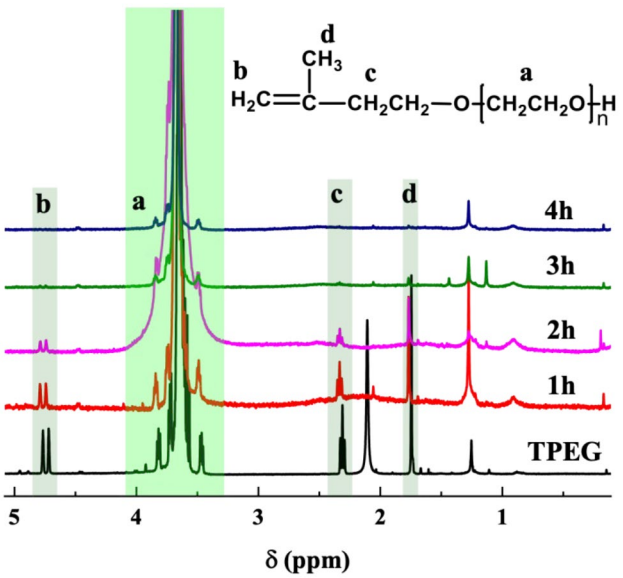

Fig. 3 [1]H-NMR spectra of TPEG and the PCE. Solvent: $CDCl_3$. Reaction conditions: [AA]: [TPEG]: [BDMAT] = 36:9:0.6, solid content is about 50%, T = 60 °C

AA monomer can be calculated using Eq. (1) based on comparison of the residual AA signals with the internal standard, trioxane (δ = 5.1 ppm). In Eq. (1), t represents the dropping time of AA, and the unit is hour, n(AA) represents the total amount of AA, n(trioxane) represents the amount of trioxane, $I_{(a+b+c)}$ represents the total integral area of the residual AA monomer at a, b, and c, and $I_{5.1}$ represents the integral area of trioxane at δ = 5.1 ppm.

Figure 3 presents the [1]H-NMR spectra of TPEG and the obtained PCE during the reaction process after evaporation of water and AA. Peak a, appeared in the range of 3.40 to 3.90 ppm, is the signal of the hydrogens in EO repeating units (CH_2CH_2-O) in TPEG, which is significantly higher than other peaks. Peak b, located at 4.80–4.70 ppm, is the signal of the hydrogens on the carbon–carbon double bond of TPEG (CH_2 = C). Peak c (2.36–2.27 ppm) and peak d (1.8–1.7 ppm) are the signals of methyl and allyl protons, respectively. With the reaction proceeding, peaks b, c, and d decreased gradually, indicating that TPEG was gradually consumed during the copolymerization. According to Eq. (2), by calculating the area ratio of peak b or c or d relative to peak a, and comparing with TPEG monomer, the conversion of TPEG can be obtained. In this formula, $I_{a,\ TPEG}$ and $I_{b,\ TPEG}$ represent the integral area of peaks a and b for TPEG macromonomer, respectively; I_a and I_b represent the integral area of peaks a and b which belong to the copolymer, respectively.

$$Con(TPEG) = \frac{I_{b,TPEG} - \frac{I_b}{I_a / I_{a,TPEG}}}{I_{b,TPEG}} \quad (2)$$

The calculated results of TPEG and AA conversion are shown in Table 2. According to the data summarized in Table 2, the monomer conversion rate in each hour is also calculated, and the results are shown in Table 3. We can clearly see that the conversion rate of TPEG gradually decreased each hour, indicating that the content of TPEG units on the PCE main chain decreased gradually with the consumption of TPEG. Meanwhile, AA is continuously dripped at a constant rate to keep the reaction going. Similarly, we can see from Table 3 that the conversion rate of AA increased each hour. As a result, the content of AA units increased gradually along the polymer backbone. Because of the symmetrical structure of BDMAT, gradient structured PCE as shown in Fig. 1a is formed: the density of TPEG units decreased along the main chain to the middle and AA units varied in the opposite direction. The composition ($\overline{F}_1 / \overline{F}_2$) of the obtained copolymers increased from 1.50 at 1 h to 2.06 at 2 h, and finally to 3.95 at 4 h, which provides direct evidence for the gradient character. Furthermore, $\overline{M}_n$ of the copolymers gradually increased with the polymerization time, and the PDIs were very small, indicating that RAFT agent has a good control over the $\overline{M}_n$ and growth of the gradient PCE. It is worthy to note that although the synthesis of gradient copolymer of PEGMA and MAA has been reported by Pourchet via RAFT copolymerization [34], the

Table 2 The conversion of AA and TPEG at different reaction times

AA (M_1) dropping time	AA conv. (%)	AA content in PCE (mol)	TPEG (M_2) Conv. (%)	TPEG content in PCE (mol)	$\bar{F}_1/\bar{F}_2$	$\overline{M}_n$(g/mol)	PDI
1 h	13.6	0.0053	36.3	0.0034	1.50	14900	1.20
2 h	30.2	0.0119	58.7	0.0055	2.06	19400	1.29
3 h	54.7	0.0224	80.8	0.0076	2.70	23200	1.30
4 h	88.5	0.0332	89.1	0.0084	3.95	24400	1.33

evolution of copolymer composition and molecular weight has not been studied in detail.

As shown in Fig. 4c, the absorption band at 2900 cm^{-1} is derived from the C-H stretching vibration of saturated hydrocarbons, and the absorption peak of ether bond (C–O–C) in the PEO long chain is at 1100 cm^{-1}. The asymmetric stretching vibration peak of C = O in the carboxyl group appears near 1640 cm^{-1}. The stretching vibration peak of C = O in AA units was constantly strengthened with the proceeding of polymerization, indicating that AA was continuously polymerized into the main chain of the macromolecule.

In order to investigate the influence of molecular weight and acid-ether ratio on the performance of PCEs, we designed and synthesized a series of gradient copolymers with different molecular weights and acid-ether ratios by adjusting the molar ratio of RAFT reagent to monomers, see Table 4 for details. PCE-1 to PCE-6 were prepared at the same acid-ether ratio (4:1) but with different molecular weights, and PCE-3, PCE-7 to PCE-10 were designed with similar molecular weights but with different acid-ether ratios. It can be seen that the PDIs of the obtained polymers are all very small, ranging from 1.1 to 1.4. These results indicate that our RAFT polymerization is well controlled. Under the same reaction conditions, we also synthesized PCEs by FRP using TGA as a chain transfer agent. From Table 5, it can be seen that the PDIs of the PCEs prepared by FRP are greater than 1.7, which is much larger than those by RAFT polymerization in Tables 2 and 4.

PCE with block structure

For the synthesis of P(TPEG-*grad*-AA)-*b*-PAA-*b*-P(AA-*grad*-TPEG) (block-1), we first prepared P(TPEG-*grad*-AA)-TTC-P(AA-*grad*-TPEG) macro-RAFT agent by RAFT polymerization process similar to those of gradient structured PCE. The ^{1}H-NMR spectrum of the macro-RAFT agent is shown in Fig. 5a. It is obvious that no signal of the double bond of AA or TPEG was observed, indicating the complete conversion of monomer in the first polymerization step. After block copolymerization of AA, $\overline{M}_n$ of the block copolymer increased from 24,000 g/mol of the macro-RAFT agent to 30,500 g/mol. Meanwhile, the PDI of the block copolymer remained very small. These results indicate that the PAA segment is successfully incorporated in P(TPEG-*grad*-AA)-TTC-P(AA-*grad*-TPEG), leading to the formation of P(TPEG-*grad*-AA)-*b*-PAA-*b*-P(AA-*grad*-TPEG) block PCE.

Table 3 The conversion rate of AA and TPEG in each hour

AA dropping time	AA conv. (%)	TPEG conv. (%)
0–1 h	13.6	36.3
1–2 h	16.6	22.4
2–3 h	24.5	12.1
3–4 h	33.8	8.3

For the synthesis of PAA-*b*-P(AA-*grad*-PEG)-*b*-PAA (Block-2), PAA-TTC-PAA macro-RAFT agent was first synthesized. The $\overline{M}_n$ of PAA-TTC-PAA was 6500 g/mol. After block copolymerization, the $\overline{M}_n$ of PAA-*b*-P(AA-*grad*-TPEG)-*b*-PAA further increased to 31,500 g/mol (see Table 6). Although the PDI of PAA-*b*-P(AA-*grad*-TPEG)-*b*-PAA became slightly larger, it was still much smaller than those of PCEs prepared by FRP in Table 5, indicating well controlled block copolymerization process. In the ^{1}H-NMR spectrum of PAA-TTC-PAA (Fig. 5b), peak a (δ = 1.25–2.05 ppm) and peak b (δ = 2.22 ppm) is corresponding to the signals of the methylene protons (-C**H**$_2$-CH-) and methine proton (-CH$_2$-C**H-)** of AA units, respectively. In the second step of block copolymerization, P(TPEG-*grad*-AA) block was successfully incorporated through copolymerization of TPEG and AA. Consequently, the peak of AA units became relatively weak as compared with the strong signal of EO units from TPEG units.

Interestingly, subtle similarities can be observed between the molecular weight data displayed in Table 6. The $\overline{M}_n$ of PAA-*b*-P(AA-*grad*-TPEG)-*b*-PAA increased by 25,000 g/mol from that of PAA-TTC-PAA, which is close to the molecular weight of P(TPEG-*grad*-AA)-TTC-P(AA-*grad*-TPEG) (24,000 g/mol), the first block of P(TPEG-*grad*-AA)-*b*-PAA-*b*-P(AA-*grad*-TPEG). Identically, from P(TPEG-*grad*-AA)-TTC-P(AA-*grad*-TPEG) to P(TPEG-*grad*-AA)-*b*-PAA-*b*-P(AA-*grad*-TPEG), the $\overline{M}_n$ increased by 6600 g/mol, which is just close to the value of PAA-TTC-PAA macro-RAFT agent (6500 g/mol). These coincidences indirectly demonstrate that the PCEs were well controlled by

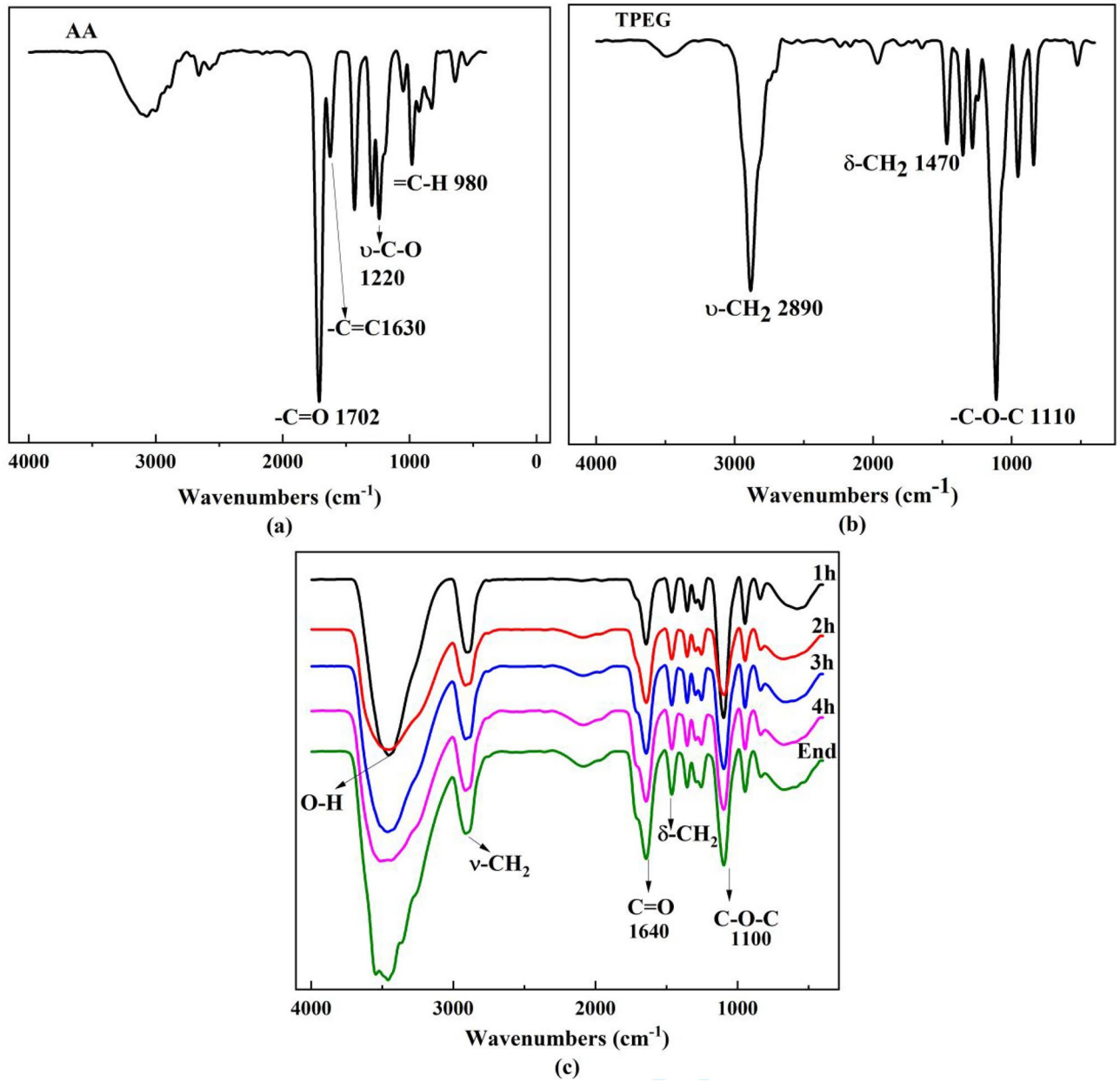

Fig. 4 FT-IR spectra of AA (**a**), TPEG (**b**), and PCE (**c**). Conditions: [AA]: [TPEG]: [BDMAT] = 36:9:0.6, solid content is about 50%, $T = 60$ °C

the RAFT polymerization, and consequently, the obtained PCEs possess the desired structure as we designed.

Adsorption study

Adsorption properties of PCEs with different molecular weights

By measuring the adsorption equilibrium curve of PCEs on the surface of cement particles, the adsorption performances of PCE with different $\overline{M}_n$ were studied systematically.

As shown in Fig. 6, the adsorbed amount of PCE on the surface of cement particles gradually increases with increasing initial PCE dosage. Besides, the adsorbed amount of dispersant on the surface of the cement particles also gradually increases with the molecular weight varied from 20,200 g/mol (PCE-1) to 27,000 g/mol (PCE-4). It is well recognized that the ionized carboxylic groups are responsible for the absorption of copolymer on cement particles. The number of ionized carboxylic groups on a single macromolecular chain increased gradually with the molecular weight of PCE, so the adsorbed amount of PCE increases accordingly. However, the adsorbed amount of PCEs decreased

Table 4 Reaction conditions and results for the synthesis of gradient PCEs by RAFT polymerization

PCE	n(AA): n(TPEG)	n(AA): n(TPEG): n(BDMAT)	$\overline{M}_n$(g/mol)	PDI
PCE-1	4:1	36:9:1.2	20200	1.24
PCE-2	4:1	36:9:1.0	22600	1.23
PCE-3	4:1	36:9:0.8	24900	1.20
PCE-4	4:1	36:9:0.7	27000	1.30
PCE-5	4:1	36:9:0.6	32600	1.30
PCE-6	4:1	36:9:0.4	34000	1.38
PCE-7	3:1	27:9:0.6	24000	1.29
PCE-8	5:1	45:9:0.6	25800	1.37
PCE-9	6:1	54:9:0.6	25700	1.34
PCE-10	7:1	63:9:0.6	28400	1.37

Table 5 Reaction conditions and results for the synthesis of PCEs by FRP

PCE	n(AA): n(TPEG)	n(AA): n(TPEG): n(TGA)	$\overline{M}_n$(g/mol)	PDI
PRE-1	4:1	36:9:0.6	31400	2.05
PRE-2	4:1	36:9:1	27700	1.74
PRE-3	6:1	54:9:1	28900	1.94

gradually when their molecular weights were higher than that of PCE-4. The reason might be that the spatial crimping degree of PCE molecules increased with increasing length of main chain [42]. As a result, the ionized carboxylic groups of PCEs with higher molecular weight will be shielded to some extent, leading to a decrease in absorbed amount. In addition, the adsorption amounts of PCE-3 and PCE-4 are much higher than that of the commercial product (Blank) with similar molecular weight, indicating that PCEs with gradient structure exhibit higher adsorption capacity as compared with random analogs.

Adsorption properties of PCEs with different structure and acid-ether ratios

To explore the effect of charge density on the adsorption performance of PCE, the adsorption equilibrium curves of PCEs with different acid-ether ratios and structure on the surface of cement particles are shown in Fig. 7.

In Fig. 7, the adsorbed amount of dispersant on the cement surface increases gradually with increasing dosage, and the adsorption equilibrium curve gradually becomes flat after reaching a certain adsorbed amount. The adsorption capacity of the PCE increases with increasing proportion of acrylic acid units in the copolymers (acid-ether ratios increases from 3:1 to 7:1). It is widely acknowledged that the charge density of the copolymers is the principal factor that determines the adsorption of PCE onto the surface of cement particles, and the greater the charge density, the higher the adsorption amount and strength [43]. Furthermore, it should be noted that the adsorption capacity of the two block PCEs is larger than that of the gradient PCE-9 with the same acid-ether ratio. This could be attributed to the concentrated distribution of anchoring anionic groups along the main chain of the block copolymers, leading to high adsorption amount of the dispersant. In these two kinds of block copolymers, the adsorption

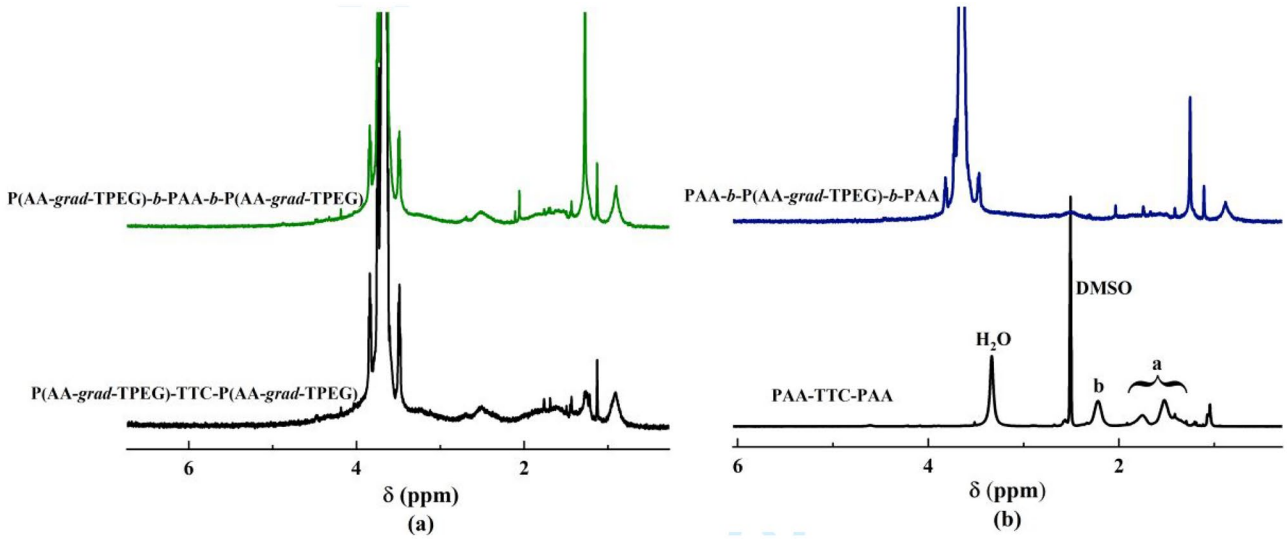

Fig. 5 ^{1}H-NMR spectra of block PCE **a** P(AA-*grad*-TPEG)-*b*-PAA-*b*-P(AA-*grad*-TPEG), **b** PAA-*b*-P(AA-*grad*-TPEG)-*b*-PAA. Solvent: PAA-TTC-PAA is in DMSO, the others are in $CDCl_3$

Table 6 Reaction conditions and results for the synthesis of block PCE by RAFT polymerization

Copolymer	n(AA): n(TPEG)	$\overline{M}_n$(g/mol)	PDI
P(AA-*grad*-TPEG)-TTC-P (AA-*grad* TPEG)	3:1	24000	1.23
P(TPEG-*grad*-AA)-*b*-PAA-*b*-P (AA-*grad* -TPEG)	6:1	30600	1.27
PAA-TTC-PAA	3:0	6500	1.18
PAA-*b*-P (AA-*grad* -TPEG)-*b*-PAA	6:1	31500	1.28

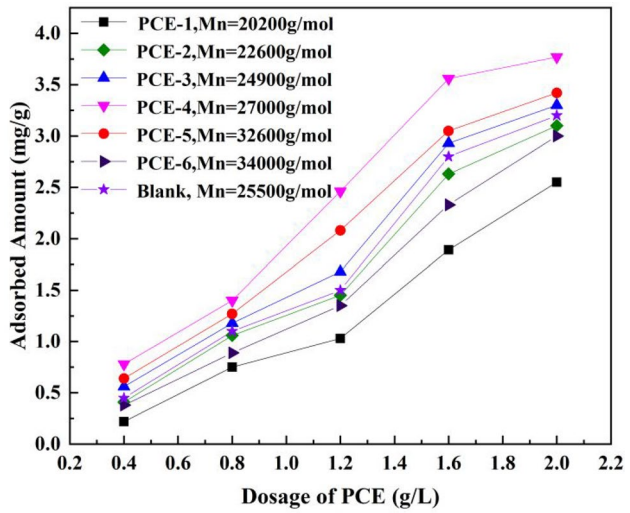

Fig. 6 Adsorption of PCEs with different molecular weight on cement pastes

capacity of the triblock copolymer with PAA block in the middle (block-1) is relatively higher, which should be ascribed to the longer length of PAA block (see Fig. 1 for the differences between them).

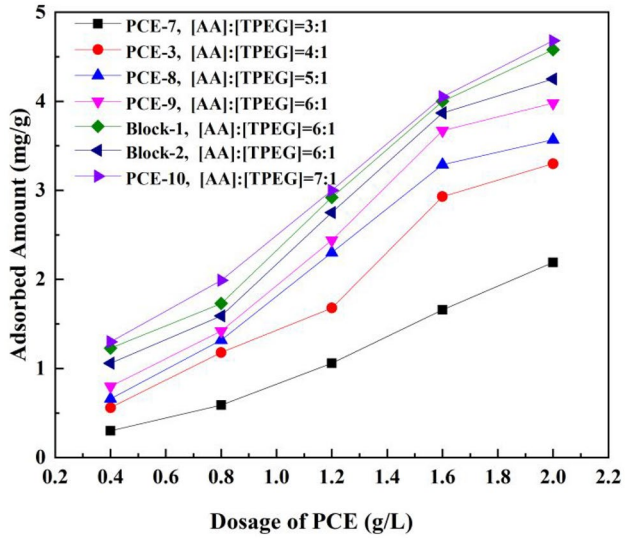

Fig. 7 Adsorption of PCEs with different structure and acid-ether ratios on cement pastes

Flowability of cement paste

Gradient PCEs

Effect of molecular weight of PCEs on fluidity of cement paste To explore the influence of molecular weight of PCEs on the fluidity of cement paste, PCEs were synthesized with different molar ratio of BDMAT to comonomers. Here, the acid-ether ratios of all the PCEs are set as 4:1. With a gradual decrease in the amount of BDMAT, the polymerization degree of the synthesized PCE increased gradually, and the $\overline{M}_n$ of PCEs increased accordingly from 20,200 g/mol for PCE-1 to 34,000 g/mol for PCE-6 (see Table 4). The fluidity of cement paste plasticized by PCEs with different molecular weights is shown in Fig. 8.

When the molecular weight of the gradient PCEs was less than that of PCE-4 ($\overline{M}_n$ = 27,000 g/mol), the initial fluidity of the cement paste increased with the increase of the molecular weight of PCEs. The initial fluidity of the cement paste with PCE-4 was the highest one: 272 mm. When the molecular weight was greater than that of PCE-4, the initial fluidity of the cement paste decreased with the increase of the molecular weight of PCEs. This trend agrees well with the absorbed amount of the PCE copolymers depicted in Fig. 6.

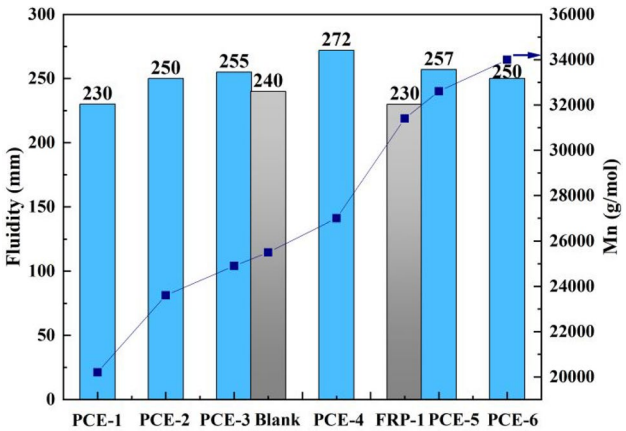

Fig. 8 Fluidity of the cement paste plasticized by PCEs with different molecular weights

When the molecular weight is relatively small, the number of ionized carboxylic groups on a single macromolecular backbone accessible for the cement particle surface is too small to be well adsorbed. With the increase of the chain length, the adsorption capacity of PCE is gradually enhanced due to increased content of ionized carboxylic groups. Meanwhile, the content of PEG side chains on a single PCE macromolecule increased accordingly, which offers spatial steric hindrance effect for the dispersion of cement particles. Thus, the dispersion of cement particles was effectively improved, and the macroscopic fluidity of the cement paste increased accordingly. However, when the molecular weight is higher than that of PCE-4, the increased spatial crimping degree of PCE resulted in a decline in the absorbed amount of PCE [42], which has been verified in Fig. 6. On the other hand, the backbones of longer PCE macromolecule may simultaneously adsorb on several cement particles, leading to the agglomeration of cement particles [44]. As a result, the fluidity decreased significantly.

It is worthy to note that the fluidity of the cement paste plasticized by PCEs with $\overline{M}_n$ in the range of 22,600 g/mol (PCE-2) to 34,000 g/mol (PCE-6) was higher than that of a commercial product synthesized by FRP (Blank, $\overline{M}_n$ = 25,500 g/mol, $PDI = 1.7$, 240 mm). We also prepared a kind of PCE by FRP with molecular weight of 31,400 g/mol (FRP-1), and the fluidity of the corresponding cement paste was 230 mm, which was about 10% lower than that of gradient PCE-5 (257 mm) with similar molecular weight ($\overline{M}_n$ = 32,600 g/mol). In addition, although the absorbed amount of PCE-2 was lower than the Blank sample (Fig. 6), the fluidity of cement paste with PCE-2 was much higher than that with the later. These results demonstrate that, as compared with PCEs with random structure synthesized by FRP, high fluidity of cement paste can be achieved by gradient PCEs with much wider range of molecular weight. The reason for the excellent fluidity of cement paste endowed by gradient PCEs will be analyzed later in comparison with the block PCEs.

Effect of acid-ether ratio of PCEs on fluidity of cement paste PCEs with different densities of carboxylic acid groups were obtained by RAFT method to study the effect of the relative content of carboxylic groups on the plasticization properties of PCEs. The fluidity of the cement paste plasticized by PCEs with different acid-ether ratios was shown in Fig. 9. When the acid-ether ratio was less than 6:1, the initial fluidity of the cement paste increased with increasing carboxylic groups content. When the acid-ether ratio was greater than 6:1, the initial fluidity of the slurry decreased with increasing acid-ether ratio.

Obviously, the charge density of the PCEs increases with increasing acid-ether ratios, and higher charge density generally leads to higher adsorption amount and strength. Therefore, the initial fluidity of the cement paste containing PCE-7 (AA: $TPEG = 3{:}1$) was very small, as the density of carboxyl group was minimal. Less content of carboxyl groups led to a smaller amount of PCE adsorbed on the cement particles (see Fig. 7), and a consequently lower fluidity. As acid-ether ratio increased, the adsorption amount increased, leading to high fluidity. When the acid-ether ratio was suitable (6:1 for PCE-9), the highest fluidity was achieved.

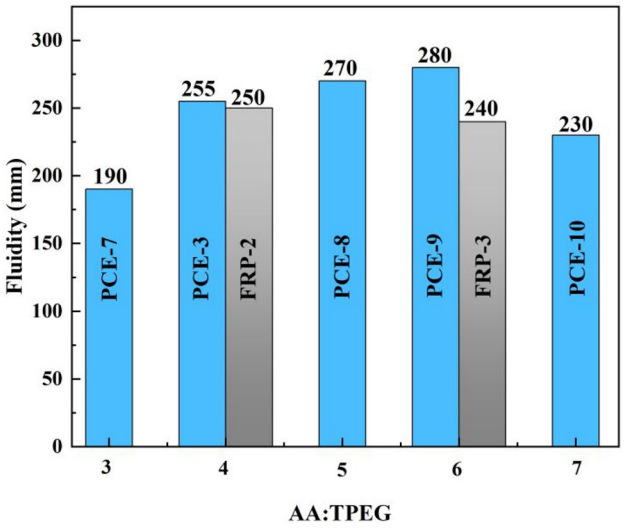

Fig. 9 Fluidity of the cement paste plasticized by PCEs with different acid-ether ratios

However, when the acid-ether ratio reaches saturation, the anionic charge density continues to increase due to the presence of excessive carboxylic acid groups. Dense concentration of ionic groups can introduce undesirable agglomeration forces between neighbor cement particles [43]. As a result, the particle network is strengthened and the number of effective molecular chains for dispersion of cement particles is reduced, leading to worse dispersion [43]. Moreover, PCE with higher charge density tends to form inter-crossing structure in high Ca^{2+} ions solution via complexation, leading to the aggregation of PCE molecules and the decline of steric hindrance [45]. Therefore, although the absorbed amount of PCE was even higher when the acid-ether ratio was higher than 6:1, the fluidity decreased dramatically.

We also synthesized PCEs with identical acid-ether ratio and similar molecular weight by FRP. It can be seen from Fig. 9 that the fluidity of PCE-3 was slightly higher than that of FRP-2 (both have acid-ether ratio of 4:1). For FRP-3 with 6:1 acid-ether ratio, the fluidity value (240 mm) was about 15% lower than that of PCE-9 (280 mm). These comparisons demonstrated that the range of acid-ether ratios for high fluidity of cement paste was broader for gradient PCEs than random analogs prepared by FRP.

Table 7 Fluidity of the cement paste with block PCEs

PCEs	Fluidity of cement paste/mm
PAA-*b*-P (AA-*grad*-TPEG)-*b*-PAA	235
P (TPEG -*grad*-AA)-*b*-PAA-*b*-P (AA-*grad*-TPEG)	118

Block PCEs

With the acid-ether ratio fixed as 6:1, we synthesized two kinds of block PCEs as shown in Fig. 1 and the detailed information of these block copolymers is presented in Table 6. It can be clearly seen from Table 7 that the fluidity of cement paste with block PCEs, especially P(AA-*grad*-TPEG)-*b*-PAA-*b*-P(AA-*grad*-TPEG), is much lower than that of gradient PCE-9 (280 mm) and FRP-3 (240 mm) with the same acid-ether ratio.

Some studies have shown that the gradient copolymer has better interface stabilization effect than the block copolymer analog [30, 31]. The research on interfacial activity and assembly behavior has demonstrated that the block copolymer is easy to form interlayer with narrower width while the gradient copolymer tends to build broader interfacial layer [46, 47]. Therefore, the gradient copolymer absorbed on the cement particles may have more stretched conformation than the block analog, thus affording high adsorption capacity onto cement particles and efficient steric hindrance simultaneously. For P(AA-*grad*-TPEG)-*b*-PAA-*b*-P(AA-*grad*-TPEG), the PAA block was located in the middle of the main chain, forming the longest PAA segment among the synthesized PCEs, which has the highest charge density. As mentioned above, although the excessively high charge density makes high adsorbed amount, the adsorption film may become multilayers and the linkage of neighbor cement particles can be formed due to the strong ionic forces within the adsorbed PCE [43]. In addition, the inter-crossing structure via complexation of COO^- with Ca^{2+} ions becomes serious with increasing charge density [45]. Therefore, P(AA-*grad*-TPEG)-*b*-PAA-*b*-P(AA-*grad*-TPEG) exhibited the lowest fluidity of cement particles. In the case of PAA-*b*-P(AA-*grad*-TPEG)-*b*-PAA, the homo-PAA block was divided into two segments as compared with P(AA-*grad*-TPEG)-*b*-PAA-*b*-P(AA-*grad*-TPEG), so the charge density was weakened. Therefore, its fluidity was higher than that of P(AA-*grad*-TPEG)-*b*-PAA-*b*-P(AA-*grad*-TPEG).

Compared with PCEs prepared by FRP, gradient PCEs prepared by RAFT exhibit better flow performance. The primary cause of excellent dispersion performance of the gradient PCEs should be the structural effect. It is well known that the molecular structure affects the adsorption behavior and steric hindrance of PCE on cement particles. In comparison to "random" PCE, a gradient distribution of the carboxylate groups leads to a higher charge density than that of the PCE by FRP, but lower than those in block architectures (see Fig. 1). Figure 10 shows the representative macromolecular composition and structure of PCE prepared by FRP. Simply put, due to the difference in reactivity between AA and TPEG and the dropwise addition of AA, the copolymer composition of the obtained PCE varied continuously during the process of FRP: in the early period, the content of TPEG units in the copolymer formed is higher, and with polymerization proceeding, the content of AA units in the obtained copolymer became higher in the late stage. In other words, the "gradient" characteristics are reflected by the macromolecules generated at different FRP periods (see Fig. 10). The copolymer generated in the early stage has high content of TPEG units but very few AA units. On the contrary, the copolymer generated in the late stage has high content of AA units. In theory, the copolymers formed in the early and late stages are not suitable for superplasticizers. According to the effect of acid-ether ratio on adsorption and fluidity of cement paste in this work and literature [43], too high or too low acid-ether ratio will reduce the dispersibility of PCEs on cement particles. The copolymer formed in the early stage of polymerization corresponds to the case of low acid-ether ratio, while the polymer formed in the late stage corresponds to the case of high acid-ether ratio. Therefore, the PCE copolymer formed in the intermediate process of FRP exhibits good properties, while the PCE copolymers generated in the early and late stages have very poor dispersibility.

The moderate charge density of gradient PCE macromolecule can take better use of anionic groups to neutralize

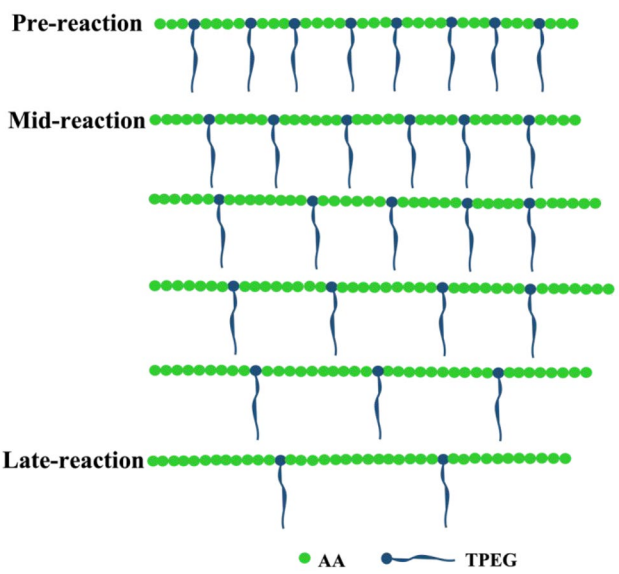

Fig. 10 Schematic representation for the random PCE synthesized by FRP

counter ions on cement particles, leading to higher adsorption amount. At the same time, PEO side chains are mainly located on exterior part of PCE macromolecule, guaranteeing the steric effect of side chains and preventing the formation of multilayer of dispersant. The appropriate balance of charge density and PEO steric stabilization effect endows the cement paste plasticized by gradient PCEs with high fluidity.

In brief, gradient PCEs have the best dispersion properties, and the PCEs with block character exhibit the lowest flowability of cement paste, while the fluidity of cement paste plasticized by PCEs with random structure is in between.

The influence of SO_4^{2-} on the dispersibility of PCEs

PCEs may encounter some problems in practical application, such as poor compatibility. Among them, cement, sand, stone, and mineral admixtures contain different types of sulfates, which have become a major factor that seriously affects the performance of PCEs. Thus, the high adaptability in complex environments is of great significance for the development of concrete admixtures. In this study, SO_4^{2-} is added to the cement, and then the fluidity of the cement paste is tested to evaluate the adaptability of the PCEs in sulfate environments.

It is clear from the data in Table 8 that the fluidity of cement paste gradually decreased with the increase of sulfate content, due to the "competitive adsorption" between PCE and SO_4^{2-} on the cement particles [48].

For gradient PCEs, when the content of Na_2SO_4 was 0.33% of cement mass, the fluidity of cement paste with PCE-3, PCE-4, PCE-5, and PCE-7 was increased compared to those without Na_2SO_4. It is explained that the low content of sulfate can increase the adsorption capacity of PCE on cement particles [49, 50]. When the sodium sulfate content further increased to 1%, the fluidity of all cement pastes began to drop drastically. Gradient PCEs with molecular weights ranged from 24,900 g/mol (PCE-3) to 32,600 g/mol (PCE-5) and acid-ether ratio from 4:1 to 6:1 showed better sulfate resistance than the products (Blank, FRP-2 and FRP-3) synthesized by FRP (the same color represents similar molecular weights). In the case of PCE-9 (27,000 g/mol), the highest fluidity was achieved among the studied PCEs (see Fig. 9) and it also showed good sulfate resistance, which highlights the charm of gradient PCE. Gradient copolymers of PEGMA and MAA reported in the work of Plank also showed high resistance to sulfate [51], and the higher anionic charge density of gradient copolymer should be the key contribution: the very strong anchoring of gradient copolymer on the surface of mineral particles weakens the competitive adsorption of sulfate. Block-2 (PAA-*b*-P(AA-*grad*-TPEG)-*b*-PAA) showed excellent resistance to sulfate. However, in the case of P(TPEG-*grad*-AA)-*b*-PAA-*b*-P(AA-*grad*-TPEG), the cementitious paste lost flowability completely when Na_2SO_4 was added. This also verify that the performance of this block PCE is poorest.

Table 8 Fluidity of the cement paste with PCEs under different sulfate content

PCE	Na_2SO_4 content/%			
	0	0.33	1.00	1.67
PCE-1	230	210	185	140
PCE-2	250	245	190	155
PCE-3	255	260	205	168
PCE-4	272	275	218	175
PCE-5	257	270	215	170
PCE-6	250	235	180	127
PCE-7	190	195	110	–[c]
PCE-8	270	260	230	177
PCE-9	280	274	245	200
PCE-10	230	195	143	–[c]
Block-1[a]	118	–	–	–
Block-2[b]	235	235	245	215
Blank	240	240	200	160
FRP-2	250	245	194	149
FRP-3	240	248	213	158

[a]Block-1 is P(TPEG-*grad*-AA)-*b*-PAA-*b*-P(AA-*grad*-TPEG)

[b]Block-2 is PAA-*b*-P(AA-*grad*-TPEG)-*b*-PAA

[c]"–" indicates that the cement paste cannot flow

In summary, the gradient PCEs with appropriate molecular weight (24,900 g/mol ~ 32,600 g/mol) and acid-ether ratios (4:1 ~ 6:1) are significantly less sensitive to the sulfate competitive adsorption.

Conclusions

PCEs with well-defined gradient and block structures were prepared by RAFT polymerization in aqueous solution, and their structures were characterized in detail. By comparing the effect of different kinds of PCEs with similar molecular weight and the same acid-ether ratio on the cement slurry fluidity and sulfate resistance, it was found that gradient PCEs had the best dispersibility, followed by random PCEs, and block PCEs showed the worst performance. The primary cause of excellent dispersion performance of the gradient PCEs should be the structural effect. The gradient distribution of AA in gradient PCE makes its charge density moderately high, leading to a large adsorption capacity on cement particles. At the same time, PEO side chains are mainly distributed on exterior part of PCE macromolecule, guaranteeing the steric effect of side chains and preventing the formation of multilayer of dispersant. In addition, we found that the gradient PCEs can achieve excellent

dispersion properties over a wide range of molecular weights (22,600 ~ 34,000 g/mol) and acid-ether ratios (4 ~ 6) as compared to random PCEs.

We envision that gradient PCEs with outstanding dispersibility will play a very important role in cement technology in the future. The properties of cement mortar and concrete modulated by gradient PCEs are under study in our lab.

Funding Science and Technology Research and Development Plan Project in Shijiazhuang, grant/award number: 201160144A.

Declarations

Conflict of interest The authors declare no competing interests.

References

1. Huang H, Qian C, Zhao F, Qu J, Danzinger GJ (2016) Improvement on microstructure of concrete by polycarboxylate superplasticizer (PCE) and its influence on durability of concrete. J Construct Build Mater 110:293–299. https://doi.org/10.1016/j.conbuildmat.2016.02.041
2. Plank J, Sakai E, Miao C, Yu C, Hong J (2015) Chemical admixtures–chemistry, applications and their impact on concrete microstructure and durability. Cem Concr Res 78:81–99. https://doi.org/10.1016/j.cemconres.2015.05.016
3. Qiu X, Peng X, Yi C, Deng Y (2011) Effect of side chains and sulfonic groups on the performance of polycarboxylate-type superplasticizers in concentrated cement suspensions. J Dispersion Sci Technol 32(2):203–212. https://doi.org/10.1080/01932691003656888
4. Aïtcin PC, Flatt RJ (2015) Science and Technology of Concrete Admixtures. Woodhead Publishing
5. Aïtcin PC (2000) Cements of yesterday and today: concrete of tomorrow. Cem Concr Res 30:1349–1359. https://doi.org/10.1016/S0008-8846(00)00365-3
6. Plank J, Bian H (2010) Method to assess the quality of casein used as superplasticizer in self-levelling compounds. Cem Concr Res 40:710–715. https://doi.org/10.1016/j.cemconres.2010.01.005
7. Uchikawa H, Hanehara S, Sawaki D (1997) The role of steric repulsive force in the dispersion of cement particles in fresh paste prepared with organic admixture. Cem Concr Res 27:37–50. https://doi.org/10.1016/S0008-8846(96)00207-4
8. Yoshioka K, Sakai E, Daimon M, Kitahara A (1997) Role of steric hindrance in the performance of superplasticizers for concrete. J Am Ceram Soc 80:2667–2671. https://doi.org/10.1111/j.1151-2916.1997.tb03169.x
9. Ren Q, Zou H, Liang M, Wang Y, Wang J (2014) Preparation and characterization of amphoteric polycarboxylate and the hydration mechanism study used in Portland cement. RSC Adv 4:44018–44025. https://doi.org/10.1039/C4RA05542J
10. Lv S, Liu J, Zhou Q, Ling H, Sun T, JI Research EC (2014) Synthesis of modified chitosan superplasticizer by amidation and sulfonation and its application performance and working mechanism. J Indus Eng Chem Res 53:3908–3916. https://doi.org/10.1021/ie403786q
11. Liu X, Guan J, Lai G et al (2017) Novel designs of polycarboxylate super plasticizers for improving resistance in clay-contaminated concrete. J Indus Eng Chem 55:80–90. https://doi.org/10.1016/j.jiec.2017.06.031
12. Liu X, Wang Z, Zhu J, Zheng Y, Cui S, Lan M (2014) Synthesis, characterization and performance of a polycarboxylate superplasticizer with amide structure. Colloids Surf 448:119–129. https://doi.org/10.1016/j.colsurfa.2014.02.022
13. Liu J, Ran Q, Miao C, Zhou D (2011) Synthesis and characterization of comb-like copolymer dispersant with methoxy poly (ethylene oxide) side chains. Polym Plast Technol 50:59–66. https://doi.org/10.1080/03602559.2010.512351
14. Salian VD, Byrne ME (2013) Living radical polymerization and molecular imprinting: improving polymer morphology in imprinted polymers. Macromol MaterEng 298:379–390. https://doi.org/10.1002/mame.201200191
15. Kuo CY, Don TM, Hsu SC, Lee CF, Chiu WY, Huang CY (2016) Thermo- and pH-induced self-assembly of P(AA-b-NIPAAm-b-AA) triblock copolymers synthesized via RAFT polymerization. J Polym Sci Part A: Polym Chem 54:1109–1118. https://doi.org/10.1002/pola.27950
16. Boussiron C, LeBechec M, Sabalot J, Lacombe S, Save M (2020) Photoactive rose bengal-based latex via RAFT emulsion polymerization-induced self-assembly. Polym Chem. https://doi.org/10.1039/d0py01128b
17. Galanopoulo P, Dugas PY, Lansalot M, D'Agosto F (2020) Poly (ethylene glycol)-b-poly (vinyl acetate) block copolymer particles of various morphologies via RAFT/MADIX aqueous emulsion PISA. Polym Chem. https://doi.org/10.1039/d0py00467g
18. Ding C, Fan C, Jiang G, Pan X, Zhang Z, Zhu ZhuJ, X, (2015) Photocatalyst-free and blue light-induced RAFT polymerization of vinyl acetate at ambient temperature. Macromol Rapid Commun 36:2181–2185. https://doi.org/10.1002/marc.201500427
19. Vishwakarma S, Kumari A, Mitra K, Singh S, Singh R, Singh J, Ray B (2019) L-menthol-based xanthate mediator for RAFT polymerization of vinyl acetate. J Macromol Sci 57:299–309. https://doi.org/10.1080/10601325.2019.1691457
20. Wolpers A, Bergerbit C, Ebeling B, D'Agosto F, Monteil V (2019) Aromatic xanthates and dithiocarbamates for the polymerization of ethylene through reversible addition-fragmentation chain transfer (RAFT). Angew Chem Int Ed 53:6683–6686. https://doi.org/10.1002/anie.201403491
21. Dommanget C, D'Agosto F, Monteil V (2014) Polymerization of ethylene through reversible addition–fragmentation chain transfer (RAFT). Angew Chem Int Ed 53:6683–6686. https://doi.org/10.1002/anie.201403491
22. Braunecker WA, Matyjaszewski K (2007) Controlled/living radical polymerization: features, developments, and perspectives. Prog Polym Sci 32:93–146. https://doi.org/10.1016/j.progpolymsci.2006.11.002
23. Nikos H, Iatroua H, Marinos P et al (2006) Macromolecular architeerctures by living and controlled/living polymerizations. Prog Polym Sci 31:1068–1132. https://doi.org/10.1016/j.progpolymsci.2006.07.002
24. Bouhamed H, Boufi S, Magnin A (2007) Dispersion of alumina suspension using comb-like and diblock copolymers produced by RAFT polymerization of AMPS and MPEG. J Colloid Interface Sci 312:279–291. https://doi.org/10.1016/j.jcis.2007.03.060
25. Fan X, Wang X, Cao M et al (2017) "Y"-shape armed amphiphilic star-like copolymer: design, synthesis and dual-responsive unimolecular micelle formation for controlled drug delivery. J Polym Chem 8:5611–5620. https://doi.org/10.1039/C7PY00999B
26. Tan M, Shi Y, Fu Z, Yang W (2018) In situ synthesis of diblock copolymer nano-assemblies via dispersion RAFT polymerization induced self-assembly and Ag/copolymer composite nanoparticles thereof. Polym Chem 9:1082–1094. https://doi.org/10.1039/c7py01905j
27. Wu Y, Tan M, Su Z, Shi Y, Fu Z, Yang W (2018) In situ synthesis of PAA-b-PSt nano-assemblies via dispersion RAFT

polymerization: effects of PEG in the medium. New J Chem 42:19353–19356. https://doi.org/10.1039/C8NJ04644A
28. Alam MM, Jack KS, Hill DJT, Whittaker AK, Peng H (2019) Gradient copolymers – preparation, properties and practice. Eur Polymer J 116:394–414. https://doi.org/10.1016/j.eurpolymj.2019.04.028
29. Kim J, Mok MM, Sandoval RW, Woo DJ, Torkelson JM (2006) Uniquely broad glass transition temperatures of gradient copolymers relative to random and block copolymers containing repulsive comonomers. Macromolecules 39:6152–6160. https://doi.org/10.1021/ma061241f
30. Sandoval RW, Williams DE, Kim J, Roth CB, Torkelson JM (2008) Critical micelle concentrations of block and gradient copolymers in homopolymer: effects of sequence distribution, composition, and molecular weight. J Polym Sci B Polym Phys 46:2672–2682. https://doi.org/10.1002/polb.21592
31. Hoogenboom R, Lambermont-Thijs HML, Jochems MJHC et al (2009) A schizophrenic gradient copolymer: switching and reversing poly(2-oxazoline) micelles based on UCST and subtle solvent changes. Soft Matter 5:3590–3592. https://doi.org/10.1039/B912491H
32. Weidmann J, Frunz L, Zimmermann J (2017) WO2017050900A1. Sika Technology AG, Switz
33. Weidmann J, Zimmermann J (2017) WO 2017050907A1. Sika Technology AG, Switz
34. Pourchet S, Liautaud S, Rinaldi D, Pochard I (2012) Effect of the repartition of the PEG side chains on the adsorption and dispersion behaviors of PCP in presence of sulfate. Cem Concr Res 42:431–439. https://doi.org/10.1016/j.cemconres.2011.11.011
35. Stecher J, Plank J (2019) Novel concrete superplasticizers based on phosphate esters. Cem Concr Res 119:36–43. https://doi.org/10.1016/j.cemconres.2019.01.006
36. Mi X, Zhang X, Ding M, Zhang M, Pei M (2021) Structure and properties of polycarboxylic acid dispersants synthesized by RAFT method. Polym Adv Technol 32:1126–1134. https://doi.org/10.1002/pat.5160
37. Yu B, Zeng Z, Ren Q, Chen Y, Liang M, Zou H (2016) Study on the performance of polycarboxylate-based superplasticizers synthesized by reversible additionefragmentation chain transfer (RAFT) polymerization. J Mol Struct 1120:171–179. https://doi.org/10.1016/j.molstruc.2016.05.035
38. Lai JT, Filla D, Shea R (2002) Functional polymers from novel carboxyl-terminated trithiocarbonates as highly efficient RAFT agents. Macromolecules 35:6754–6756. https://doi.org/10.1021/ma020362m
39. GB/T 8077–2012 (2012) Methods for testing uniformity of concrete admixture. Standardization Administration of the People's Republic of China
40. Zhang Z, Wang Z, Ren J et al (2015) Determination of monomer reactivity ratios for acrylic comb copolymer AA-TPEG. Journal of Shanxi University (Natural Science Edition) 38:332–334. https://doi.org/10.13451/j.cnki.shanxi.univ(nat.sci.).2015.02.022
41. Yin DJ (2016) Research on comonomer activity of polycarboxylate [D]. Beijing University of Technology
42. Vovk A, Vovk G, Usherov-Marshak A (1997) Regularities of hydration and structure formation of cement pastes in the presence of superplasticizers with different molecular mass. ACI Symp Publication 173:763–780
43. Javadi A, Jamil T, Abouzari-Lotf E, Soucek M, Heinz H (2021) Working mechanisms and design principles of comb-like polycarboxylate ether superplasticizers in cement hydration: quantitative insights for a series of well-defined copolymers. ACS Sustain Chem Eng 9:8354–8371. https://doi.org/10.1021/acssuschemeng.0c08566
44. Kong F, Pan L, Wang C et al (2016) Effects of polycarboxylate superplasticizers with different molecular structure on the hydration behavior of cement paste. Constr Build Mater 105:545–553. https://doi.org/10.1016/j.conbuildmat.2015.12.178
45. Tian H, Kong X, Su T, Wang D (2019) Comparative study of two PCE super-plasticizers with varied charge density in Portland cement and sulfoaluminate cement systems. Cem Concr Res 115:43–58. https://doi.org/10.1016/j.cemconres.2018.10.003
46. Beginn U (2008) Gradient copolymers. Colloid Polym Sci 286:1465–1474. https://doi.org/10.1007/s00396-008-1922-y
47. Shull KR (2002) Interfacial activity of gradient copolymers. Macromolecules 35:8631–8639. https://doi.org/10.1021/ma020698w
48. Yamda K, HANAHRA S (2001) Interaction mechanism of cement and superplasticizers: the roles of polymer adsorption and ionic conditions of aqueous phase. Concr Sci Eng 3:135–145
49. Wang Z, Jiang N, Wang Y et al (2012) Influence of sulfate on adsorption capability and kinetics of polycarboxylate type superplasticizer. J Chin Ceram Soc 40:1586–1591. https://doi.org/10.14062/j.issn.0454-5648.2012.11.010
50. Han S, Yan P, An M (2014) Compatibility of superplasticizers in cement paste with low sulfate content. J Chin Ceram Soc 42:981–988. https://doi.org/10.7521/j.issn.04545648.2014.08.05
51. Plank J, Winter C (2008) Competitive adsorption between superplasticizer and retarder molecules on mineral binder surface. Cem Concr Res 38:599–605. https://doi.org/10.1016/j.cemconres.2007.12.003